Science in China Series B: Chemistry

Springer

www.scichina.com
chem.scichina.com
www.springerlink.com

Preparation of novel bovine hemoglobin surface-imprinted polystyrene nanoparticles with magnetic susceptibility

LI Lin[1,2], HE XiWen[1], CHEN LangXing[1†] & ZHANG YuKui[1,3]

[1] College of Chemistry, Nankai University, Tianjin 300071, China;
[2] College of Pharmaceutical Sciences, Nankai University, Tianjin 300071, China;
[3] Dalian Institute of Chemical Physics, Chinese Academy of Sciences, Dalian 116011, China

In this research, a surface imprinting strategy has been adopted in protein imprinting. Bovine hemoglobin surface-imprinted polystyrene (PS) nanoparticles with magnetic susceptibility have been synthesized through multistage core-shell polymerization system using 3-aminophenylboronic acid (APBA) as functional and cross-linking monomers. Superparamagnetic molecularly imprinted polystyrene nanospheres with poly(APBA) thin films have been synthesized and used for the first time for protein molecular imprinting in an aqueous solution. The magnetic susceptibility is imparted through the successful encapsulation of Fe_3O_4 nanoparticles. The morphology, adsorption, and recognition properties of superparamagnetic molecularly imprinted polymers (MIPs) have been investigated using transmission electron microscopy, X-ray diffraction, thermogravimetric analysis, and vibrating sample magnetometer. Rebinding experimental results show that poly(APBA) MIPs-coated superparamagnetic PS nanoparticles have high adsorption capacity for template protein bovine hemoglobin and comparatively low nonspecific adsorption. The imprinted superparamagnetic nanoparticles could easily reach the adsorption equilibrium and achieve magnetic separation in an external magnetic field, thus avoiding some problems of the bulk polymer.

magnetic nanoparticles; protein molecular imprinting; poly(3-aminophenylboronic acid) thin films; selective adsorption

1 Introduction

The molecular imprinting technique (MIT) is a kind of promising method for imparting a predetermined molecular recognition property onto tailored materials that can recognize and in some cases respond to biological and chemical agents of interest[1−3]. In contrast to biological counterparts, enzymes, and antibodies, molecularly imprinted polymers (MIPs) display significant advantages of high mechanical/chemical stability, low cost, easy preparation, and predictable specific recognition. MIT is widely applicable to the separation media[4], mimicking antibody[5], chemical and biochemical sensing[6], and drug delivery[7].

In recent years, magnetic nanoparticles (MNPs) play a more and more important role in the fields of biomedical and biotechnological applications, including magnetic resonance imaging (MRI) contrast enhancement, target drug delivery, and separation and purification of proteins and cells[8,9], because of their small size and high surface-to-volume ratio. Compared with those of the conventional micrometer-size resins or beads, MNPs have many superior characteristics for bioseparation applications, such as good dispersability, fast and effective

Received April 25, 2009; accepted May 18, 2009
doi: 10.1007/s11426-009-0182-0
†Corresponding author (email: lxchen@nankai.edu.cn)
Supported by the National High-Tech Research & Development Program of China (Grant No. 2007AA10Z432), the National Basic Research Program (Grant No. 2007CB914100), the National Natural Science Foundation of China (Grant Nos. 20675040 & 20875050), and the Natural Science Foundation of Tianjin (Grant No. 07JCYBJC00500)

binding of biomolecules, and reversible and controllable flocculation[10]. Moreover, the power and efficiency of magnetic separation is especially useful for the large-scale operations[11]. Surface modification of MNPs is a key to many of these applications. The selectivity of MNPs can be improved by MIPs film on the surface, which possesses specific affinities for guest molecules[1−3]. When modified with a specific functional polymer, for example, the MIPs, which provide functional materials able to recognize and in some cases respond to biological and chemical agents of interest, these MNPs coated MIPs could be used to separate and concentrate chemicals more conveniently with the help of an external magnetic field.

However, most of the successes in molecular imprinting are based on small target ligands, whereas the imprinting of macromolecules like proteins has been proven more problematic. Some difficulties faced by these large molecules in the imprinting application lie in the entrapment of the macromolecular template in the polymer matrix, poor mass transfer, low integrity of the polymer structure, and the production of heterogeneous binding sites, due to the geometric and chemical complexity of proteins[12,13]. To solve these problems associated with bulk templates, surface imprinting has been proposed as a viable strategy for protein imprinting, which conduces to the ease of template removal as well as uptake. An ultrathin polymer coating on a solid support substrate through the surface imprinting approach can improve the mass transfer and reduce permanent entrapment of protein template, but these methods also reduce the number of imprint sites[14−22]. To overcome the difficulty, nanosized matrix is one of the important directions of development, that is, to make MIPs not only allow the prompt diffusion of proteins but also have enough binding area.

3-Aminophenylboronic acid (APBA) is an attractive functional monomer for protein imprinting, due to its water-solubility. It provides a mild aqueous medium during polymerization, and offers a variety of favorable and reversible interactions with amino acids on the protein. The ultrathin poly(APBA) films have been fabricated as surface coatings on solid support substrate such as polystyrene microwell plate and microsphere, glass slide, and gold surface of quartz crystal microbalance (QCM) electrode[14,17−20]. Poly(APBA) can be easily synthesized through the chemical oxidation of 3-aminophenylboronic acid and can be grafted tightly to the surface of polystyrene (PS) microtiter plates by aromatic ring electron-pairing interactions[23].

Hence, the combination of the advantages of magnetic separation with those of molecular imprinting would ideally provide a more effective technique with characteristics of simplicity, flexibility, and selectivity. By incorporating magnetic iron oxide, the superparamagnetic composite MIP beads with an average diameter of 13 μm were prepared using suspension polymerization in perfluorocarbon for the first time[24]. Recently, protein surface-imprinted submicrometer particles with magnetic susceptibility through miniemusion polymerization were reported[22]. We reported the synthesis of Fe_3O_4 magnetic nanoparticles coated estrone-imprinted polymer with controlled size using a semi-covalent imprinting strategy[25], and poly(APBA) thin films were coated onto the silica-modified Fe_3O_4 surface through surface imprinting[26]. In this paper, we propose a novel synthesis of core-shell bovine hemoglobin (BHb) imprinted magnetic nanoparticles. The morphology, adsorption, and recognition properties of magnetic molecularly imprinted nanomaterial were investigated, and the application of magnetic molecularly imprinted nanoparticles in the field of protein separation and enrichment were initially attempted. Our studies indicate that poly(APBA) can be tightly grafted onto the surfaces of PS nanospheres and that PS nanospheres with imprinted poly(APBA) have a specific selectivity for the initially imprinted protein.

2 Methods

2.1 Materials

3-Aminophenylboronic acid monohydrate was obtained from Beijing Element Chem.-Tech. Company (Beijing, China). Ammonium persulphate (APS, $(NH_4)_2S_2O_8$), NaOH, $NaHCO_3$, and Tween-20 were obtained from Tianjin North Tianyi Chemical Reagent Factory (Tianjin, China). Styrene, hexadecane (HD), sodium dodecyl sulfate (SDS), and ethanol were purchased from the Tianjin Guangfu Fine Chemical Research Institute (Tianjin, China). 3-Methacryloxy(propyl)trimethoxysilane (WD-70) was purchased from Hubei Wuda organic silicone materials Co., LTD (Hubei, China). Styrene was washed with NaOH aqueous solution (5%, w/w) for several times to remove inhibitor. Bovine serum albumin (BSA,

MW 68 kDa, pI = 4.9) was obtained from Beijing Dingguo Bio.-Tech. Company (Beijing, China). BHb (MW 68 kDa, pI = 6.8—7.2) was obtained from Shanghai Lanji Chem. -Tech. Company (Shanghai, China). Deionized water was used in all experiments.

All the other materials were of analytical grade and commercially available, including $FeCl_3 \cdot 6H_2O$, $FeCl_2 \cdot 4H_2O$, NH_4OH (25%, w/w), tetraethyl orthosilicate (TEOS), and 2-propanol.

2.2 Synthesis of superparamagnetic magnetite nanoparticles

An aqueous suspension of superparamagnetic magnetite nanoparticles was prepared through the controlled chemical coprecipitation reaction[27]. $FeCl_2 \cdot 4H_2O$ (3.44 g) and $FeCl_3 \cdot 6H_2O$ (9.44 g) were separately dissolved in deaerated deionized water (160 mL) under a N_2 atmosphere with vigorous mechanical stirring (800 rpm). A nitrogen gas environment was maintained in the vessel during the reaction to prevent critical oxidation. When the solution was preheated to 80℃, NH_4OH (20 mL) was added to achieve alkaline conditions. After 30 min, the black superparamagnetic MNPs were obtained through sedimentation with help of an external permanent magnet and the supernatant was decanted. The MNPs were washed with deionized water for several times (150 mL each time) to remove unreacted chemicals until the stable ferrofluid was obtained.

2.3 Synthesis of superparamagnetic silica nanoparticles

The superparamagnetic MNPs were coated with silica by using a sol-gel method. 120 mg of superparamagnetic MNPs were redispersed in 240 mL of 2-propanol and 18 mL of deionized water by sonication for approximately 15 min. Then under continuous mechanical stirring (800 $r \cdot min^{-1}$), 21 mL of NH_4OH and 4 mL of TEOS were consecutively added to the reaction mixture in the vessel. The reaction proceeded at room temperature for 14 h under continuous mechanical stirring. The resultant product was obtained through magnetic separation with help of an external permanent magnet and was thoroughly washed with deionized water.

2.4 Synthesis of superparamagnetic polystyrene nanoparticles

The superparamagnetic PS nanoparticles were synthesized through surface modification and grafting. Briefly, superparamagnetic silica nanoparticles containing WD-70 and ethanol were mixed under continuous mechanical stirring (800 $r \cdot min^{-1}$). After 3 h, the solution was heated to 70℃ for 2 h. The resultant product was obtained through magnetic separation with help of an external permanent magnet and was thoroughly washed with deionized water and ethanol separately.

Surface-modified nanoparticles (0.055 g) were dispersed in 1.81 g of styrene and 0.1 g of hexadecane by sonication for approximately 20 min. Subsequently, 0.1 g SDS (0.1 g), $NaHCO_3$ (0.0015 g), and deionized water (10 g) were added to the solution in a nitrogen gas environment at room temperature with vigorous mechanical stirring (800 $r \cdot min^{-1}$). After 30 min, the solution became fine emulsion by sonication for approximately 15 min and then was added to 7.5 mg APS in a nitrogen gas environment at 70℃ for 3 h.

2.5 Synthesis of MIP or NIP

In the preparation of BHb-imprinted polymer, 10.0 mg BHb was dissolved in 5 mL sodium phosphate buffer (pH 7.2) containing 100 $mmol \cdot L^{-1}$ APBA and 0.1% Tween-20 (as a surfactant), and the complex was incubated at room temperature for 1 h. After 40.0 mg superparamagnetic PS nanoparticles were added, the solution was then incubated at room temperature for 2 h. Prior to use, the superparamagnetic PS nanoparticles were subjected to extensive deionized water, and washed thoroughly. Subsequently, 6.5 mL 100 $mmol \cdot L^{-1}$ APS aqueous solution as initiator was slowly admixed dropwise with the above solution for about 20 min, and the polymerization process was executed at room temperature. After 14 h, BHb imprinted polymer were obtained. Finally, the template-containing MIP-coated PS nanoparticles were washed with 0.2 $mol \cdot L^{-1}$ sodium phosphate buffer (pH 9.0) containing 0.5 $mol \cdot L^{-1}$ sorbitol to remove the entrapped template molecules. The MIP-coated PS nanoparticles were then equilibrated with the buffer used in the polymerization.

NIP was prepared via the same procedure in the absence of BHb.

2.6 Characterization of synthesized nanoparticles

The size and morphology of the nanoparticles were measured by a FEI (Netherlands) Tecnai-20 transmission electron microscopy (TEM). The nanoparticle sample dispersed in hexane solution was cast onto a carbon-

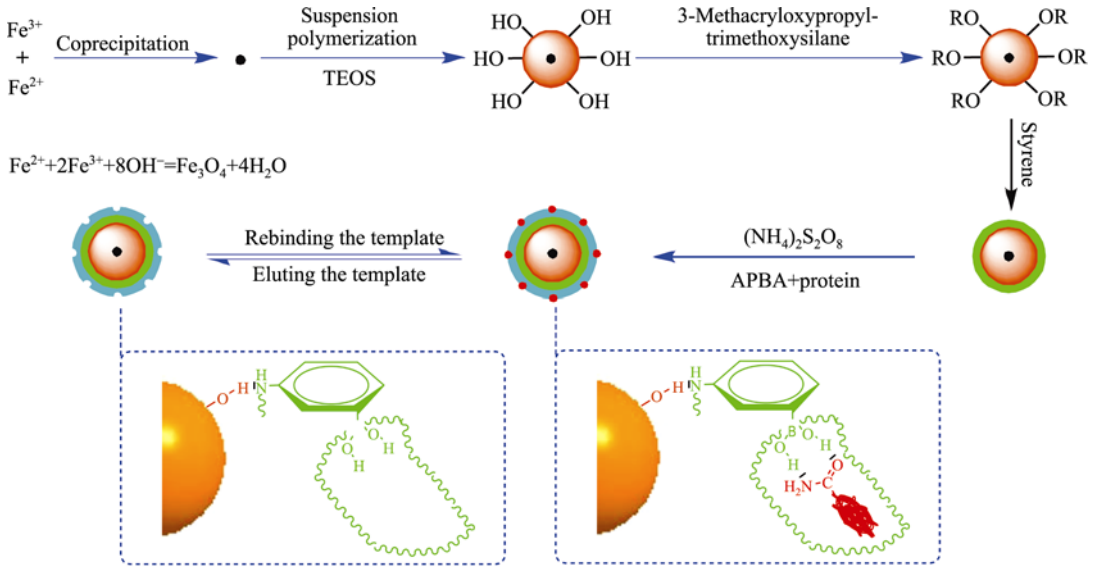

Figure 1 Schematic illustration of the preparation of magnetic molecularly imprinted nanoparticles.

coated copper grid sample holder and was evaporated at room temperature.

Thermogravimetric analysis (TGA) was performed for powder samples (~10 mg) with a heating rate of 10℃·min^{-1} using a Netzsch STA 409 (Germany) thermogravimetric analyzer under a nitrogen atmosphere up to 1000℃.

The crystal structure of nanoparticles was determined by X-ray diffraction (XRD). The XRD pattern of each sample was recorded with a Shimadzu (Japan) D/Max-2500 diffractometer, using a monochromatized X-ray beam with nickel-filtered Cu Kα radiation. The XRD patterns were collected in the range of $5° < 2\theta < 80°$ with a dwelling time of 2 s and a scan rate of 6.0°·min^{-1}. The substance is automatically searched by using JCPDS-International Center for Diffraction Data.

Magnetic properties were measured with a vibrating sample magnetometer (VSM) (LDJ9600-1, USA) at room temperature.

2.7 Protein adsorption experiments

Rebinding conditions were kept the same as synthesis conditions. The amount of the protein adsorbed onto the MIP-coated PS nanoparticles was calculated from the differences in the protein concentrations before and after incubation on the rotator (100 r·min^{-1}). The protein concentrations were measured with a Shimadzu (Japan) UV-2450 spectrophotometer at 405 nm for BHb. The eluting solution was prepared by admixing an 80 mL 0.5 mol·L^{-1} sorbitol aqueous solution with a 20 mL 0.2 mol·L^{-1} sodium phosphate buffer (pH 9.0). Before eluted, the nanoparticles were washed thoroughly with deionized water to remove the non-adsorbed protein.

The experimental data are presented as the adsorption capacity per unit mass (mg) of the nanoparticles, and the adsorption capacity (Q) is calculated as follows:

$$Q = (C_0 - C_s) \times V / m \quad (1)$$

Here C_0 (mg·mL^{-1}) is the initial concentration of protein solution; C_s (mg·mL^{-1}) is the protein concentration of the supernatant; V (mL) is the volume of the initial solution; m (mg) is the mass of the nanoparticles.

3 Results and discussion

3.1 Synthesis of MIP-coated MNPs

The synthesis of the MIP-coated MNPs via a multistep procedure is illustrated in Figure 1, which involves synthesis of Fe_3O_4 MNPs, silica-shell deposition, surface modification, PS grafted onto silica surface, poly(APBA) film onto the PS surface, final extraction of template protein, and generation of the recognition site. It is known that the critical particle size of superparamagnetism of magnetic particles is 25 nm. Therefore, the prepared magnetic Fe_3O_4 nanoparticles have to be smaller than 25 nm to ensure that they have superparamagnetic properties. The formation of a silica coating on the surfaces of iron oxide nanoparticles could provide good biocompatible, non-toxic coating as well as a hydrophilic surface, and prevent their aggregation in liquid[28,29]. The growth of silica shells on Fe_3O_4 nanoparti-

cles was developed through a sol-gel process using tetraethyl orthosilicate (TEOS)[29]. The poly(APBA) thin films were coated onto the PS layer of magnetic nanoparticles through molecular imprinting process. APBA is the functional and cross-linking monomer. In an aqueous medium, template protein and functional monomer APBA form a complex through interactions between $-B(OH)_2$ group on APBA and amino acids on the template protein[14]. Due to poly(APBA) polymer is easily synthesized by chemical oxidation of APBA and can be grafted tightly to the surface of polystyrene microsphere[17] and microplate[18] by way of aromatic ring electron-pairing interactions. After washed with 0.2 $mol \cdot L^{-1}$ sodium phosphate buffer (pH 9.0) containing 0.5 $mol \cdot L^{-1}$ sorbitol till no template protein was monitored, the MIP-coated MNPs with imprinted recognition sites on the layer of the MNPs was obtained.

3.2 Characterization of the size of MNPs

TEM images of magnetite, magnetite@silica, silica-coated MNPs with WD-70, PS-coated MNPs, and poly (APBA) MIP-coated MNPs are illustrated in Figure 2. From these images, it is obvious that all of these particles remain nanosized and have roughly spherical shape before and after being encapsulated by silica, PS, and APBA. Figure 2(a) shows the TEM image of the naked Fe_3O_4 nanoparticles. This image reveals a homogeneous size distribution with a mean diameter of about 12 nm. Figure 2(b) shows the TEM image of the magnetite@silica nanoparticles with a mean diameter of about 450 nm, which clearly shows that the magnetite nanoparticles were fully coated by the silica, providing magnetite core with a silica surface which favors the encapsulation of MNPs by polymers. Figure 2(c) shows silica nanoparticles with WD-70 have a fuzzy outline, which is due to silica surface modified by WD-70. Figure 2(d) shows that the fuzzy outline of nanoparticles in Figure 2(c) has disappeared after PS are coated onto the silica surface. The clear core-shell structure poly(APBA) thin film coated PS nanoparticles is observed from Figure 2(e). The TEM image (Figure 2(e)) shows that the poly(APBA) MIP coated magnetic PS nanoparticles retain the morphology of the original particles. The magnetic PS core is completely coated with the poly(APBA) thin films' shells in the thickness range of 15—20 nm. It is worth noting that the surfaces of the nanoparticles are porous. This image also suggests that the core-shell nanoparticles with more regular morphological features can be prepared through a step-by-step coating procedure. Moreover, the images reveal that the coating process did not significantly result in agglomeration and change in the size of particles, which is because the reaction occurred only on the particle surface. The particle size increases slightly after the coating with APBA, with a mean diameter of about 480 nm, which is larger than that of silica-coated MNPs.

3.3 Thermogravimetric analysis of MNPs

TGA was performed to further estimate the relative composition of the nano-core and the organic shell (Figure 3). All samples displayed a similar mass-loss profile for the release of physically adsorbed solvent or water and organic capping materials. The evaporation amount of solvent or water release corresponds to approximately 7% at $T < \sim 120$℃. For the organic mass loss at ~300℃ $< T < \sim 700$℃, the PS nanoparticles with poly(APBA) revealed a slightly high organic mass release of approximately 10% for the organic shell, including WD-70 and PS. This compound was completely decomposed at temperature above 700℃ and the silica coating began to slowly decompose. Both the magnetite content and silica coating content of the MNPs were evaluated to be approximately 83%. From the above TGA analysis, the coating of the silica shell to Fe_3O_4 MNPs indeed was quite efficient for the improvement of their stability and activity for further application.

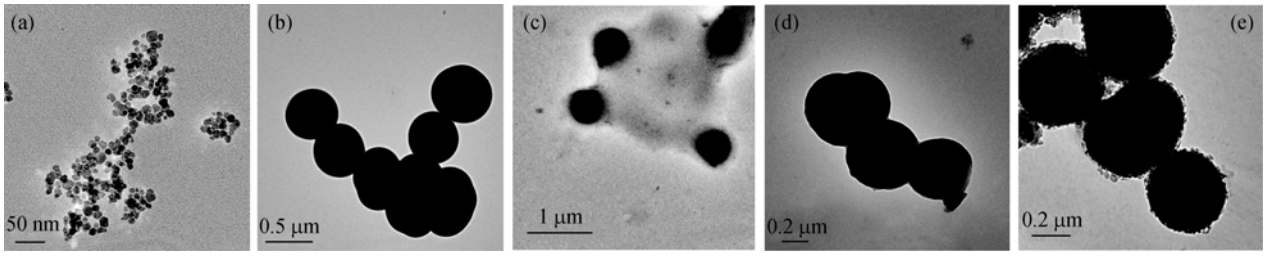

Figure 2 TEM images of (a) Fe_3O_4 MNPs, (b) silica-coated MNPs, (c) silica-coated MNPs with WD-70, (d) PS-coated MNPs and (e) poly(APBA)-coated MNPs.

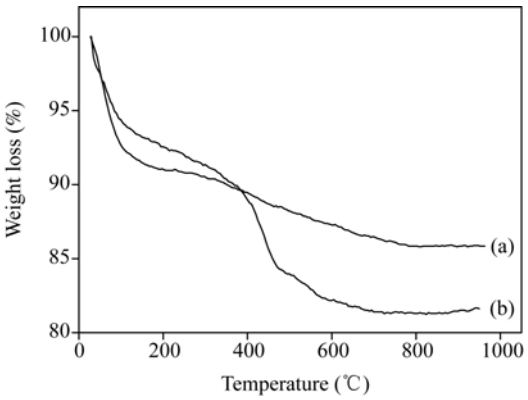

Figure 3 TGA of (a) silica-coated MNPs and (b) PS-coated nanoparticles.

3.4 X-ray diffraction analysis of MNPs

The crystal structures of the pure Fe_3O_4, silica-coated, PS-coated, and MIP-coated MNPs were investigated using Shimadzu D/Max-2500 diffractometer. As shown in Figure 4, in the 2θ range of 20—70°, there are six characteristic peaks of four MNPs with and without coating, which is quite similar to those of Fe_3O_4 nanoparticles (2θ=30.1°, 35.5°, 43.1°, 53.4°, 57.0°, and 62.6°) reported by other group. The peak positions at corresponding 2θ value are indexed as (220), (311), (400), (422), (511), and (440), respectively, which match well with the database of magnetite in JCPDS-International Center for Diffraction Data (JCPDS Card:19-629).

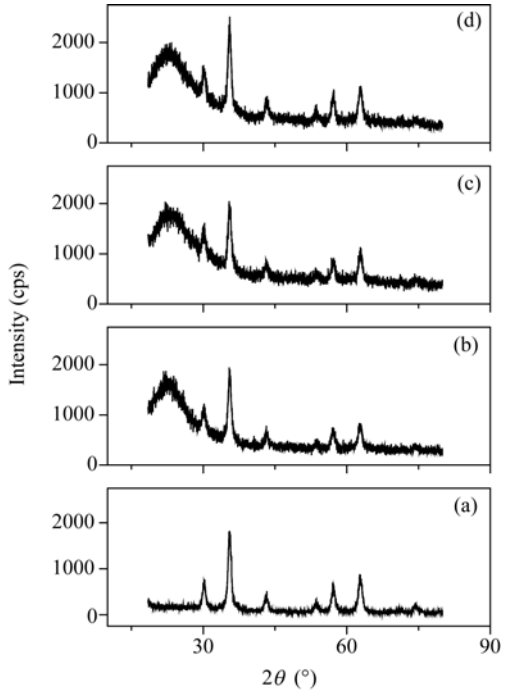

Figure 4 XRD patterns of (a) Fe_3O_4 MNPs, (b) silica-coated MNPs, (c) silica-coated MNPs with WD-70, and (d) PS-coated MNPs.

The diffraction peaks are labeled with the indexed Bragg reflections spectra of the Fe_3O_4 structure. However, XRD analysis cannot discriminate between magnetite (Fe_3O_4) and its oxidation product maghemite (γ-Fe_2O_3) because both diffraction patterns overlap and are nearly identical. There are probably two types of iron oxide particles in the dispersion: magnetite and maghemite. The XRD patterns show the presence of the characteristic diffraction peaks of magnetite/maghemite for the synthesized particles, which are highly crystalline materials. The XRD patterns also reveal that the synthesized particles contain Fe_3O_4 with a spinel structure[32] and the binding process did not result in the phase change of Fe_3O_4. Even if we may have a mixture of both the oxides, because of the fact that both these oxides are magnetic and the surface states of either phase allow the growth of a silica shell, it is not considered important to determine the relative percentages of these phases in these samples. The peak positions are unchanged while their widths have increased, indicating that the crystal structure is substantially unchanged. The intensity of the XRD peaks decreased after the particles were coated with substance because of the effect of the increasing shell.

3.5 Magnetic properties of MNPs

Vibrating sample magnetometer was employed to study the magnetic properties of the synthesized MNPs. The magnetic hysteresis loop of the dried samples at room temperature are illustrated in Figure 5. From the VSM data, the remanent magnetization (*M*r) and coercivity (*H*c) can be determined. The values of *M*r and *H*c are 1.673 emu·g^{-1} and 20.26 Oe for naked MNPs, 0.2614 emu·g^{-1} and 15.81Oe for silica-coated MNPs, 0.2418 emu·g^{-1} and 11.68 Oe for PS-coated MNPs, and 0.2659 emu·g^{-1} and 14.23 Oe for poly(APBA)-coated MNPs, respectively. The very weak hysteresis confirms that naked MNPs, silica-coated MNPs, PS-coated MNPs, and poly(APBA) MIP-coated MNPs have superparamagnetic properties at room temperature, which implies that the sample keeps no remanence in the absence of an external magnetic field. Because Fe_3O_4 and γ-Fe_2O_3 have similar magnetic properties, the oxidation of a little amount of Fe_3O_4 to γ-Fe_2O_3 during the silanization process is not important in the present study. The superparamagnetism prevents MNPs from aggregating and enables them to redisperse

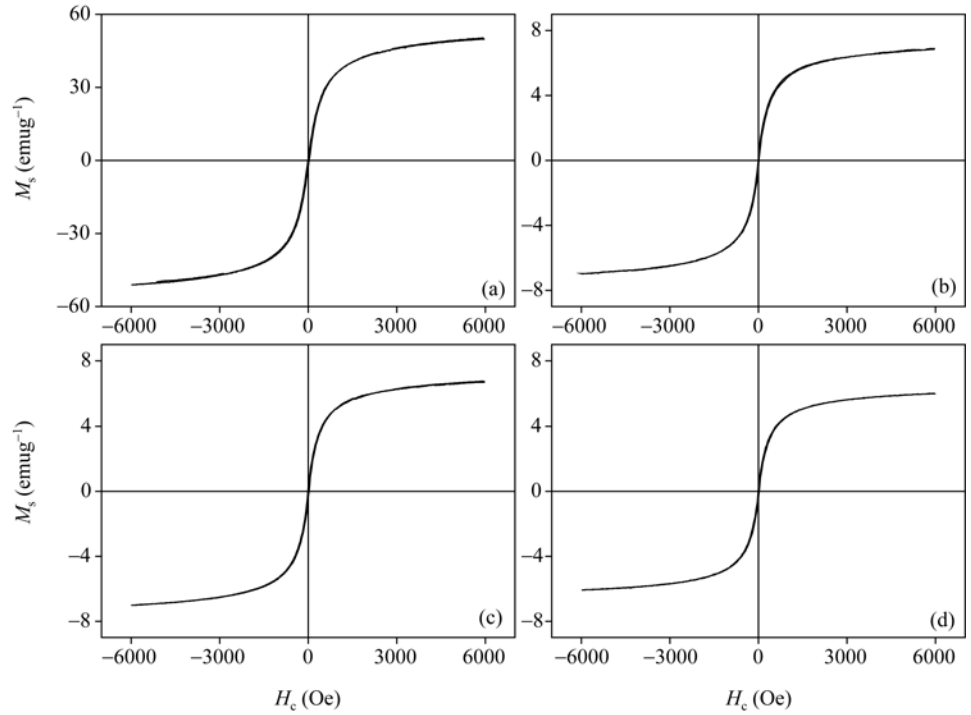

Figure 5 Hysteresis loops of (a) Fe_3O_4 MNPs, (b) silica-coated MNPs, (c) PS-coated MNPs, and (d) poly(APBA)-coated MNPs.

rapidly when the magnetic field is removed. This is because the magnetic core is so small (with an average particle size of 12 nm) that it may be considered to have a single magnetic domain.

The saturation magnetization of silica-coated MNPs, PS-coated MNPs, and poly(APBA) MIP-coated MNPs is 6.994, 6.938, and 6.057 emu·g^{-1}, respectively, which were lower than that of the naked Fe_3O_4 MNPs (50.69 emu·g^{-1}). The *M*s value for poly(APBA) MIP-coated MNPs is slightly lower than that for silica-coated MNPs and that for PS-coated MNPs. These results indicate that the surface modification has much impact on the magnetism of nanospheres, which might quench the magnetic moment. Due to such high saturation magnetization which makes them very susceptible to magnetic fields, the nanoparticles could be easily and quickly separated from a suspension. This is very favorable for the magnetic separation of proteins on a large scale.

3.6 Adsorption analysis

To investigate the affinity of MIP-coated MNPs for template BHb, binding experiments and subsequent Scatchard analysis were carried out. As a primary examination of MIP and NIP MNPs, a kinetic experiment was carried out to confirm that template can be rebound in the MIP and NIP matrix and to estimate how long it takes to reach the binding equilibrium. The MIP and NIP were incubated with 0.2 mg·mL^{-1} BHb solution for a certain time at room temperature. The amount of BHb bound to MNPs with MIP and NIP coating was plotted as a function of time and the results are shown in Figure 6(a). It can be seen that the adsorption capacity increased with time and the imprinted MNPs had high adsorption rate. In the early 60 min, the adsorption increased quickly and then slowly, and after 60 min the adsorption almost reached equilibrium. This time profile indicates an initial rapid increase in the adsorption capacity and then a slower approach to a limiting value. For the imprinted nonthin films, it takes generally 12—24 h to reach the equilibrium of adsorption[26]. However, the imprinted thin films need only 30—120 min to reach the equilibrium of adsorption for biomacromolecule templates. Therefore, in our case, it was easy for BHb molecules to reach the surface imprinting cavities of MIP, and it took less time to gain adsorption saturation, which implies that poly(APBA) MIP-coated MNPs have the property of good mass transport and thus overcome some drawbacks of the traditional monolithic imprinted materials.

To examine the controlling mechanism of the adsorption process such as mass transfer and chemical reaction,

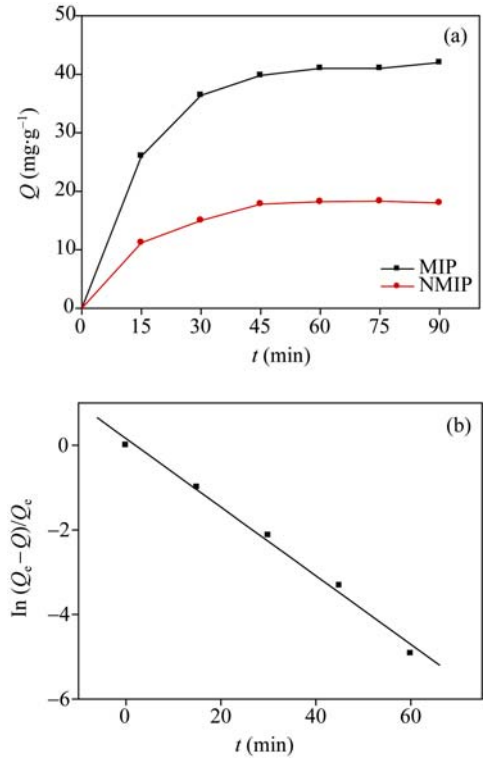

Figure 6 (a) Curve of adsorption kinetics (C_{BHb}=0.2 mg·mL^{-1}; m_{MIP}=m_{NIP}=15.0 mg; pH 7.2; T=25℃); (b) plot of ln(Q_e-Q)/Q_e vs. t.

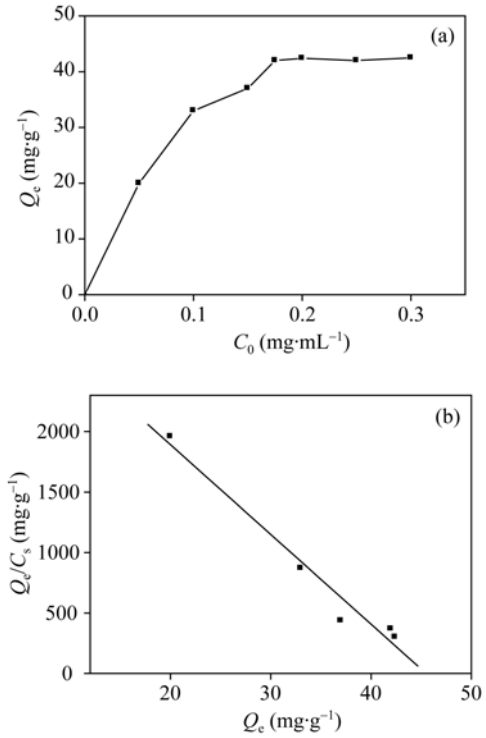

Figure 7 (a) Curve of adsorption isotherm (m_{MIP}=30.0 mg; pH 7.2; T=25℃); (b) curve of Q_e/C_s vs. Q_e.

kinetic models were used to test experimental data. The first-order rate equation of Lagergren is one of the most widely used for the adsorption of solute from a liquid solution. The BHb rebinding process can be described as an apparent pseudo first-order kinetic process[32]:

$$\ln\left(Q_e - Q\right)/Q_e = -kt \tag{2}$$

Here Q_e and Q are the final equilibrium adsorption capacity and the actual adsorption capacity, respectively. A plot of ln(Q_e–Q)/Q_e vs. t would be a straight line (Figure 6(b)) to confirm the applicability of the kinetic model. The linear regression equation is ln(Q_e–Q)/Q_e = $0.1609 - 0.0811t$ ($R^2 = 0.9914$). The apparent rate constant characterizing the speed of protein adsorption was found to be 8.11×10^{-2} from the slope of the line.

The adsorption isotherm of MIP-coated MNPs was determined in the concentration range of BHb from 0 to 0.3 mg·mL^{-1}(initial concentration). As shown in Figure 7(a), the amount of BHb bound to the MIP-coated MNPs at equilibrium Q_e increased with the increase of the initial concentration of BHb, and reached saturation at higher BHb concentration. The saturation binding data were further processed with Scatchard equation to estimate the binding properties of MIPs[33]. The Scatchard relationship can be obtained using the following equation.

$$Q_e/C_s = \left(Q_{max} - Q_e\right)/K_D \tag{3}$$

Here, Q_{max} is the saturated adsorption capacity, Q_e is the amount of BHb bound to MIPs at equilibrium, C_s is the free concentration after adsorption equilibrium, and K_D is the dissociation constant. As shown in Figure 7(b), the Scatchard plot is a single straight line, which illustrates that there is only a class of binding sites populated in MIP-coated MNPs. The linear regression equation is $Q_e/C_s = -74.23\ Q_e + 3376.7$ ($R^2 = 0.9673$). The Q_{max} and K_D are calculated to be 45.49 mg·g^{-1} and 0.0135 mg·mL^{-1}, respectively, from the slope and the intercept of the Scatchard plot. It is attractive that this kind of nanoparticles has high adsorption capacity for template protein, which is infrequent in the related literature.

3.7 Binding specificity of BHb MIP-coated MNPs

To confirm the selective recognition of the MIP-coated MNPs, we selected BSA as control. BSA is most representative and appropriate because the molecular weight and volume of BSA molecule are similar to those of BHb molecule. To test the selective recognition of MIP, the amount of BHb and BSA bound to MIP and NIP were determined by equilibrium binding experiments.

The specificity of the MIP-coated MNPs was estimated by the imprinting factor (α) of BHb-MIP, which is defined as the ratio of adsorption quantities of BHb-MIP to that of NIP ($\alpha = Q_{MIP}/Q_{NIP}$). The separation factor (β) of BHb-MIP was selected to validate the selectivity of BHb-MIP and NIP for BHb and BSA, which is defined as the ratio of adsorption quantity of template (BHb) to that of competitor molecules (BSA) ($\beta = Q_{BHb}/Q_{BSA}$). The imprinting factor α and the separation factor β were calculated from the binding data. α and β is 2.322 and 1.977, respectively. Both α and β of BHb-MIP are larger than those of using silica-coated MNPs as matrix in our former work[26]. It is suggested that, for BHb-MIP, its adsorption quantity of BHb is more than that of the competitor protein in the same solution. The experimental results (Figure 8) show that specific recognition sites for BHb formed during the course of imprinting and thin films of imprinted MNPs are able to selectively adsorb template proteins.

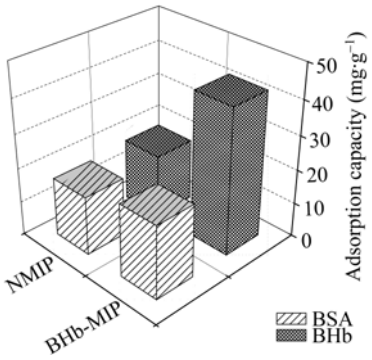

Figure 8 Adsorption selectivity of BHb-MIP and NIP for BHb and BSA, respectively ($C_{BHb} = C_{BSA} = 0.2$ mg·mL^{-1}; $m_{MIP} = m_{NMIP} = 15.0$ mg; pH 7.2; $T = 25$℃; $t = 3$ h).

4 Conclusions

A novel core-shell structure MIP-coated MNPs was prepared by coating thin films of functional monomer APBA onto the surface of PS MNPs in an aqueous medium with BHb as the templates. This kind of surface-imprinted polystyrene MNPs with magnetic susceptibility is more robust and reusable because poly (APBA) can be grafted tightly to the surface of PS layer through aromatic ring electron-pairing interactions. The morphology, adsorption, and recognition properties of superparamagnetic molecularly imprinted nanomaterials were investigated by TEM, XRD, TGA, and VSM. The experimental results show that surface-imprinted MNPs have high adsorption capacity for template protein bovine hemoglobin and comparatively low nonspecific adsorption. The imprinted MNPs could easily reach the adsorption equilibrium and achieve magnetic separation in an external magnetic field, thus avoiding some problems of the bulk polymer. In this research, we demonstrated that molecularly imprinted MNPs are applicable to the separation and detection of biomacromolecules especially for removal of high abundance of protein and enrichment of low abundance of protein in proteomics.

1 Wulff G. Molecular imprinting in cross-linked materials with the aid of molecular templates—a way towards artificial antibodies. Angew Chem Int Ed, 1995, 34: 1812—1832

2 Yan M, Ramström O. Molecularly Imprinted Materials: Science and Technology. New York: CRC Press, 2005

3 Ye L, Mosbach K. Molecular imprinting: Synthetic materials as substitutes for biological antibodies and receptors. Chem Mater, 2008, 20: 959—868

4 Zhang H, Ye L, Mosbach K. Non-covalent molecular imprinting with emphasis on its application in separation and drug development. J Mol Recognit, 2006, 19: 248—259

5 Wulff G. Enzyme-like catalysis by molecularly imprinted polymers. Chem Rev, 2002, 102: 1—28

6 Haupt K, Mosbach K. Molecularly imprinted polymers and their use in biomimetic sensors. Chem Rev, 2000, 100: 2495—2504

7 Alvarez-Lorenzo C, Concheiro A. Molecularly imprinted polymers for drug delivery. J Chromatogr B, 2004, 804: 231—245

8 Gupta A K, Gupta M. Synthesis and surface engineering of iron oxide nanoparticles for biomedical applications. Biomaterials, 2005, 26: 3995—4021

9 Zhao Z L, Bian Z Y, Chen L X, He X W, Wang Y F. Synthesis and surface-modifications of iron oxide magnetic nanoparticles and applications on separation and analysis. Prog In Chem, 2006, 18: 1288—1297

10 Lee K S, Lee I S. Decoration of superparamagnetic iron oxide nanoparticles with Ni^{2+}: Agent to bind and separate histidine-tagged proteins. Chem Commun, 2008, 709—711

11 O'Brien S M, Thomas O R T, Dunnill P. Non-porous magnetic chelator supports for protein recovery by immobilised metal affinity adsorption. J Biotechnol, 1996, 50: 13—25

12 Turner N W, Jeans C W, Brain K R, Allender C J, Hlady V H, Britt D W. From 3D to 2D: A review of the imprinting of proteins. Biotechnol Prog, 2006, 22: 1474—1489

13 Zhou X, Li W Y, He X W, Chen L X, Zhang Y K. Recent advances in

the study of protein imprinting. Sep Puri Rev, 2007, 36: 257—283
14 Turner N W, Liu X, Piletsky S A, Hlady V, Britt D W. Recognition of conformational changes in β-lactoglobulin by molecularly imprinted thin films. Biomacromolecules, 2007, 8: 2781—2787
15 Kempe M, Glad M, Mosbach K. An approach towards surface imprinting using the enzyme ribonuclease A. J Mol Recognit, 1995, 8: 35—39
16 Shi H Q, Tsai W B, Garrison M D, Ferrari S, Ratner B D. Template-imprinted nanostructured surfaces for protein recognition. Nature, 1999, 398: 593—597
17 Yan C L, Lu Y, Gao S Y. Coating lysozyme molecularly imprinted thin films on the surface of microspheres in aqueous solutions. J Polym Sci Polym Chem, 2007, 45: 1911—1919
18 Bossi A, Piletsky S A, Piletska E V, Righetti P G, Turner A P F. Surface-grafted molecularly imprinted polymers for protein recognition. Anal Chem, 2001, 73: 5281—5286
19 Chou P C, Rick J, Chou T C. C-reactive protein thin-film molecularly imprinted polymers formed using a micro-contact approach. Anal Chim Acta, 2005, 542: 20—25
20 Bonini F, Piletsky S, Turner A P F, Speghini A, Bossi A. Surface imprinted beads for thr recognition of human serum albumin. Biosens Bioelectron, 2007, 22: 2322—2328
21 Shiomi T, Matsui M, Mizukami F, Sakaguchi K. A method for the molecular imprinting of hemoglobin on silica surfaces using silanes. Biomaterials, 2005, 26: 5564—5571
22 Tan C J, Chua H G, Ker K H, Tong Y W. Preparation of bovine serum albumin surface-imprinted submicrometer particles for with magnetic susceptibility through core-shell miniemulsion polymerization. Anal Chem, 2008, 80: 683—692
23 Bossi A, Piletsky S A, Piletska E V, Righetti P G, Turner A P F. Surface-grafted molecularly imprinted polymers for protein recognition. Anal Chem, 2001, 73: 5281—5286
24 Ansell R J, Mosbach K. Magnetic molecularly imprinted polymer beads for using drug radioligand binding assay. Analyst, 1998, 123: 1611—1616
25 Wang X, Wang L Y, He X W, Zhang Y K, Chen L X. A molecularly imprinted polymer-coated nanocomposite of magnetic nanoparticles for estrone recognition. Talanta, 2009, 78: 327—332
26 Li L, He X W, Chen L X, Zhang Y K. Preparation of core-shell magnetic molecularly imprinted polymer nanoparticles for recognition of bovine hemoglobin. Chem Asian J, 2009, 4: 286—293
27 Yamaura M, Camilo R L, Sampaio L C, Macêdo M A, Nakamura M, Toma H E. Preparation and characterization of (3-aminopropyl)-triethoxysilane-coated magnetic nanoparticles. J Magn Magn Mater, 2004, 279: 210—217
28 Mornet S, Grasset F, Portier J, Duguet E. Maghemite@silica nanoparticles for Biological applications. Eur Cells Mater, 2002, 3: 110—113
29 Liu X Q, Ma Z Y, Xing J M, Liu H Z. Preparation and characterization of amino-silane modified superparamagnetic silica nanospheres. J Magn Magn Mater, 2004, 270: 1—6
30 Wang C Y, Zhu G M, Chen Z Y, Lin Z G. The preparation of magnetite Fe3O4 and its morphology control by a novel arc-electrodeposition method. Mater Res Bull, 2002, 37: 2525—2529
31 Ye L, Cormack P A G, Mosbach K. Molecularly imprinted monodisperse microspheres for competitive radioassay. Anal Commun, 1999, 36: 35—38
32 Yin G, Liu Z, Zhan J, Ding F X, Yuan N J. Impacts of the surface charge property on protein adsorption on hydroxyapatite. Chem Eng J, 2002, 87: 181—186
33 Shea K J, Spivac D A, Sellergren B. Polymer complements to nucleotide bases. Selective binding of adenine derivatives to imprinted polymers. J Am Chem Soc, 1993, 115, 3368